

# Interaction of Polyelectrolytes with Salivary Pellicles on Hydroxyapatite Surfaces under Erosive Acidic Conditions

Alice Delvar,<sup>†,‡,§</sup> Liselott Lindh,<sup>‡,||</sup> Thomas Arnebrant,<sup>†,‡</sup> and Javier Sotres<sup>\*,†,‡</sup>

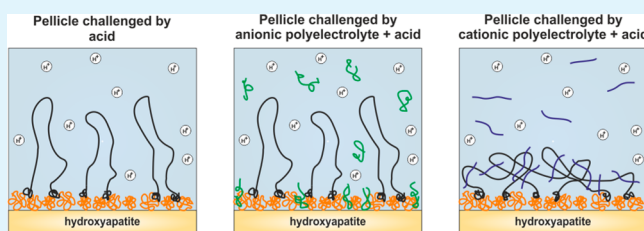
<sup>†</sup>Biomedical Science, Faculty of Health and Society, <sup>‡</sup>Biofilms-Research Center for Biointerfaces, and <sup>||</sup>Prosthetic Dentistry, Faculty of Odontology, Malmö University, 20506 Malmö, Sweden

<sup>§</sup>Chemistry Department, ENSIACET, 31030 Toulouse, France

## S Supporting Information

**ABSTRACT:** The modification of acidic beverage formulations with food-approved, nonhazardous substances with antierosive properties has been identified as a key strategy for counteracting the prevalence of dental erosion, i.e., the acid-induced dissolution of hydroxyapatite (HA, the main mineral component of tooth surfaces). While many of such substances have been reported, very little is known on how they interact with teeth and inhibit their acid-induced dissolution. With the aim of filling this gap in knowledge, we have studied under acidic conditions the interaction between two polyelectrolytes of differing ionic character, carboxymethyl cellulose (CMC) and chitosan, and saliva-coated hydroxyapatite, i.e., a model for the outer surface of teeth. These studies were performed by means of ellipsometry, quartz crystal microbalance with dissipation monitoring, and atomic force microscopy. We also studied, by means of pH variations, how dissolution of saliva-coated HA is affected by including these polyelectrolytes in the erosive solutions. Our results confirm that salivary films protect HA from acid-induced dissolution, but only for a limited time. If the acid is modified with CMC, this polyelectrolyte incorporates into the salivary films prolonging in time their protective function. Eventually, the CMC-modified salivary films are removed from the HA surfaces. From this moment, HA is continuously coated with CMC, but this offers only a weak protection against erosion. When the acid is modified with the cationic chitosan, the polyelectrolyte adsorbs on top of the salivary films. Chitosan-modified salivary films are also eventually replaced by bare chitosan films. In this case both coatings offer a similar protection against HA dissolution, which is nevertheless notably higher than that offered by CMC.

**KEYWORDS:** dental erosion, saliva, pellicle, hydroxyapatite, polyelectrolytes



## INTRODUCTION

Dental erosion, i.e., the acid-induced wear of dental hard tissue, is currently recognized in many Western countries as the main factor responsible for tooth wear.<sup>1</sup> It results not only in esthetic, orthodontic, and functional complications, but is also associated with sensitivity and pain for the patient.<sup>2</sup> Dental erosion has its origin in the tendency of hydroxyapatite (HA), the main mineral component of enamel and dentine, to dissolve under acidic conditions.<sup>3</sup> The fact is that the oral cavity is regularly exposed to acidic challenges. These can be of bacterial origin, leading to caries, but also derived from the ingestion of (extrinsic) acids or from the influx of (intrinsic) acidic stomach content, leading to dental erosion. If it were not for the secretion of saliva into the oral cavity, acid-induced erosion would eventually end up with all teeth. However, saliva is supersaturated with respect to different phases of calcium phosphate salts, allowing remineralization processes.<sup>4</sup> Saliva also counteracts erosion by diluting, neutralizing, and buffering acids.<sup>4</sup> Additionally, salivary components adsorb on tooth surfaces forming a protective layer, the pellicle, which confers acid resistance properties.<sup>5</sup> Thus, preservation of tooth

structure relies on a delicate equilibrium between erosion, protection, and mineralization processes.

Traditionally, the prevalence of dental erosion has been small.<sup>6</sup> However, this prevalence has become alarmingly high and continues to escalate.<sup>7–10</sup> Because of this, it is expected that dental erosion will have a major economic impact on dental services in the decades to come. Thus, it is not daring to place dental erosion as one of the biggest challenges in dentistry for the 21st century.

The increasing prevalence of dental erosion is associated with different aspects of modern lifestyle. Among them, the escalating consumption of acidic soft drinks stands out.<sup>11</sup> Attempts toward moderating their consumption have been proved unsuccessful so far. Thus, great efforts are being taken to modify their formulation so as to reduce their harmful effects. Increasing their pH or adding calcium and phosphate ions are not practicable options as both result in flavor deterioration.<sup>12</sup> Adding fluoride to soft drinks, even though

Received: August 3, 2015

Accepted: September 14, 2015

Published: September 14, 2015

being a successful approach,<sup>11</sup> is forbidden in most Western countries due to the risk of fluorosis. In fact, because of health concerns, plenty of research is devoted nowadays to find food-approved, nonhazardous substances with antierosive properties. At present, a high number of such compounds have been reported.<sup>13–17</sup> However, there is an alarming lack of knowledge of the mechanisms by which these compounds slow down the erosion of tooth surfaces under acidic conditions. As a consequence, it is currently not possible to design a priori strategies for finding novel and improved formulations for protecting teeth from acidic challenges.

With the aim of filling this gap in knowledge, we present a study on the interaction between polyelectrolytes widely used in the food industry and saliva-coated HA under acidic conditions, and on how this interaction influences HA acid-induced dissolution. Moreover, we hypothesized that both aspects would be strongly affected by the ionic character of the polyelectrolytes. Thus, this work focused on two polyelectrolytes of differing ionic character: the anionic carboxymethyl cellulose (CMC) and the cationic chitosan.

## MATERIALS AND METHODS

**General.** All water used was of ultrahigh quality (UHQ), processed in an Elgastat UHQ II apparatus (Elga Ltd., High Wycombe, Bucks, England). All chemicals used were of at least analytical grade.

**Erosive Challenges.** We studied the effect of exposing clean (noncoated) and pellicle-coated HA surfaces to three different erosive challenges (ECs), i.e., acidic solutions. For the first erosive challenge (EC1), 0.3% (w/v) citric acid (reference C1909, Sigma-Aldrich, St. Louis, MO, USA) solution containing no further additions was used. For the second erosive challenge (EC2), a carboxymethyl cellulose (CMC) in citric acid solution was used. For this purpose sodium carboxymethyl cellulose (MW 250 kDa, DS 0.7, reference 419311, Sigma-Aldrich, St. Louis, MO, USA) was dissolved in the 0.3% (w/v) citric acid solution to a 0.02% (w/v) CMC concentration. For the third erosive challenge (EC3), a chitosan in citric acid solution was used. Specifically, an initial stock solution consisting of 0.5% (w/v) chitosan (MW 550 kDa, DD 75%, reference 50494, Sigma-Aldrich, St. Louis, MO, USA) in 1% (v/v) acetic acid was prepared and left for stirring for 12 h. Then, this stock solution was further diluted 10-fold in UHQ water and citric acid added to reach concentrations of 0.3% (w/v) for citric acid and of 0.05% (w/v) for chitosan. Finally, the pH of all solutions was adjusted to a value of 3.2 by using NaOH (Sigma-Aldrich, St. Louis, MO, USA).

**Saliva Collection.** Stimulated human whole saliva was collected from one healthy adult male donor by chewing Parafilm and drooling into a chilled tube. Collection was performed in the morning at least 2 h after breakfast and oral hygiene procedures. The freshly collected saliva was immediately used without further treatments. The donor gave his informed consent to participate in the study, which was approved by the regional ethical review board in Lund, Sweden (2010/649).

**QCM-D.** Quartz crystal microbalance with dissipation (QCM-D) measurements were performed by using an E4 system (Q-Sense AB, Sweden). A detailed description of the technique and its basic principles can be found elsewhere.<sup>18</sup> Briefly, an alternating-current voltage is applied through a gold-coated quartz chip to stimulate the shear mode oscillation of the quartz crystal. Adsorption of a certain amount of mass onto the sensor surface leads to a decrease in the frequency of the resonance overtones,  $f_{\nu}$ ,<sup>19</sup> although it is not straightforward to establish the correct relationship between both quantities when dealing with viscoelastic materials.<sup>20</sup> Additionally, the coupled mass sensed in QCM-D experiments includes that of the adsorbed film and that of the coupled solvent.<sup>21,22</sup> Thus, it is often referred as “wet mass”. Along with the shifts in  $f_{\nu}$ , QCM-D is able to detect changes in the dissipation factor,  $D_{\nu}$ , of each of the overtones.<sup>23</sup> The dissipation factor represents the ratio between the energy

dissipated by the sensor during a single oscillation after switching off the driving voltage and the initial oscillation energy of the sensor.

Specifically, the sensors used in QCM-D experiments (from now on HA1 surfaces, Model QSX327, Q-sense AB, Sweden) consisted of a monolayer of HA nanoparticles (thickness ca. 10 nm) deposited onto gold-coated AT-cut piezoelectric quartz crystals via a titanium layer (thickness ca. 50 nm). Previous studies have shown that the deposited HA preserves its crystalline structure.<sup>24</sup> These surfaces are highly planar, with AFM imaging revealing an average surface roughness of  $\sim 1$  nm (Supporting Information, section S1). Before measurements, HA1 surfaces were first rinsed with ethanol, then rinsed extensively with water, treated in a Hellmanex II 1% (v/v) in water solution, and finally rinsed extensively with water, ethanol, and water again. Finally, before being used, the HA1 surfaces were dried under nitrogen and plasma-cleaned for 5 min in low pressure residual air using a glow discharge unit (PDC-32 G, Harrick Scientific Corp., USA).

QCM-D experiments consisted of the following steps during which the cell was thermostated to 22 °C, and the frequency and dissipation were constantly monitored: (i) filling the liquid cell with PBS buffer pH 7.4 and waiting until stable frequency and dissipation signals were observed, (ii) flowing saliva (0.2 mL·min<sup>-1</sup>) through the liquid cell until it completely replaced the PBS buffer ( $\sim 2$  min), (iii) allowing saliva adsorption for 1 h under nonflow conditions, (iv) flowing PBS buffer (0.2 mL·min<sup>-1</sup>) for 5 min, (v) stabilization of the sample for 45 min, (vi) flowing the erosive solution to be tested (0.2 mL·min<sup>-1</sup>) for 5 min, (vii) stabilization under nonflow conditions for 35 min, (viii) flowing PBS buffer (0.2 mL·min<sup>-1</sup>) for 5 min, and (ix) stabilization under nonflow conditions for 35 min. QCM-D results are expressed as a mean and a deviation from the mean values calculated from a set of two experiments.

**Ellipsometry.** Ellipsometry<sup>25</sup> was also employed to study the effect of the different erosive challenges on HA pellicles. The experimental setup was based on null ellipsometry according to the principles of Cuyper.<sup>26</sup> The instrument used was a Rudolph thin film ellipsometer (type 43603-200E, Rudolph Research, USA) automated according to the concept of Landgren and Jönsson.<sup>27</sup> A xenon arc lamp was used as the light source, and light was detected at 442.9 nm using an interference filter with UV and infrared blocking (Melles Griot, The Netherlands). The trapezoid cuvette made of optical glass (Hellma, Germany) was equipped with a magnetic stirrer and thermostated to 22 °C.

For ellipsometry experiments we used the same type of HA surfaces (HA1) that were used for QCM-D experiments. Cleaning of the HA1 surfaces was performed in the same way as well. Ellipsometry experiments consisted of the following steps which mimic those of QCM-D experiments: (i) filling the cuvette with PBS buffer pH 7.4 and waiting until stable frequency and dissipation signals were observed, (ii) flowing saliva through the cuvette until it completely replaced PBS buffer while stirring, (iii) stopping flow and stirring and allowing saliva adsorption for 1 h, (iv) flowing PBS buffer for 5 min while stirring, (v) stabilization under nonflow and nonstirring conditions for 45 min, (vi) flowing with the erosive solution to be tested for 5 min while stirring, (vii) stabilization under nonflow and nonstirring conditions for 35 min, (viii) flowing PBS buffer for 5 min while stirring, and (ix) stabilization under nonflow and nonstirring conditions for 35 min.

The analysis of ellipsometry data obtained from experiments on HA surfaces is not straightforward as HA and proteins (the pellicle is mostly a proteinaceous film) possess similar refractive indices. When this is the case, the resolution of the ellipsometry raw data, i.e., the ellipsometry angles, is low. Nevertheless, the adsorbed amount (from now on also named as “dry mass”, as it does not take into account the solvent coupled to the film) can still be determined by imposing a reasonable value to the refractive index of the adsorbed layer.<sup>28–31</sup>

Before saliva adsorption, four-zone measurements were performed in PBS buffer in order to calculate the effective complex refractive index,  $n_{\text{eff}}^* = n_{\text{eff}} - i\kappa_{\text{eff}}$ , of the HA1 surfaces, for which a two-layer model was employed. The average and standard deviation values of these quantities obtained from the measurements performed for all sensors used in this work were  $n_{\text{eff}} = 1.90 \pm 0.11$  and  $\kappa_{\text{eff}} = 2.47 \pm 0.14$ .

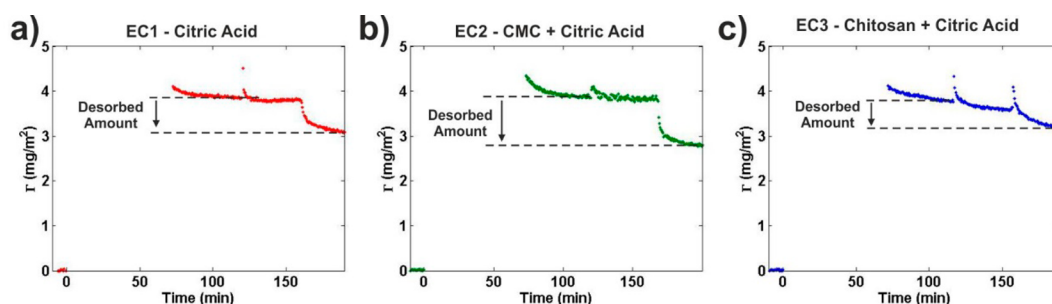


**Figure 1.** Time evolution of the adsorbed amount (dry mass) of HA1 pellicles when exposed to (a) EC1, (b) EC2, and (c) EC3 challenges. Data for  $t < 0$  min corresponds to the baseline acquired in PBS buffer. In the time range 0–60 min the HA1 surface was in contact with whole saliva leading to the formation of the pellicle (no data was recorded in this time interval because of the high absorbance/scattering of bulk saliva). In the time range 60–110 min the pellicles were rinsed with PBS buffer. In the time range 110–150 min the pellicles were exposed to the erosive challenges. Finally, in the time range 150–190 min the challenged pellicles were rinsed again with PBS buffer.

**Table 1.** Relative Change in Dry Mass (Determined by Ellipsometry and Characterized by the Parameter  $R_{\text{DryMass}}$ ), Wet Mass (Determined from Frequency Shifts Measured by QCM-D and Characterized by the Parameter  $R_{\text{WetMass}}$ ), Viscoelasticity (Determined by QCM-D and Characterized by the Parameter  $R_{\text{viscoelasticity}}$ ), and Mechanical Stability (Determined by AFM Scratching Experiments and Characterized by the Parameter  $R_{\text{strength}}$ ) of Pellicles Exposed to Different Erosive Challenges with Respect to Pellicles before Being Exposed to Erosive Challenges

	$R_{\text{DryMass}}$	$R_{\text{WetMass}}$	$R_{\text{viscoelasticity}}$	$R_{\text{strength}}$
EC1: citric acid	$0.79 \pm 0.01$	$0.98 \pm 0.01$	$1.02 \pm 0.07$	$0.78 \pm 0.08$
EC2: CMC + citric acid	$0.75 \pm 0.04$	$0.90 \pm 0.01$	$1.03 \pm 0.02$	$1.31 \pm 0.17$
EC3: chitosan + citric acid	$0.83 \pm 0.01$	$1.17 \pm 0.04$	$0.93 \pm 0.05$	$0.66 \pm 0.06$

These values differ from those expected for HA surfaces ( $n \sim 1.6$ ), indicating a notable contribution from the underlying Ti and Au layers. For the calculation of the adsorbed amounts of the pellicles (before and after being exposed to erosive challenges), a three-layer model (solution–pellicle–HA sensor) was used and the de Feijter formula was employed.<sup>25,32</sup> For this, the refractive index of the pellicles (before and after erosion) was set to 1.45,<sup>33</sup> the refractive index of the solvent was set to 1.344, and the increase of the adsorbate refractive index with the concentration was set to  $0.18 \text{ mL} \cdot \text{g}^{-1}$ . Ellipsometry results are expressed as a mean and a deviation from the mean values calculated from a set of two experiments.

**AFM Imaging.** A commercial atomic force microscope equipped with a liquid cell (MultiMode 8 SPM with a NanoScope V control unit; Bruker AXS, Santa Barbara, CA, USA) was employed to visualize HA1 pellicles. For this purpose, HA1 surfaces were incubated in human whole saliva for 1 h, and subsequently rinsed with PBS buffer. Samples were then immediately placed on the AFM for visualization, not allowing them to dry at any moment. Afterward, samples were immersed in the solution corresponding to a given erosive challenge for 40 min, then thoroughly rinsed with PBS buffer, and immediately placed in the AFM for visualization. AFM imaging was performed at room temperature ( $\sim 22^\circ \text{C}$ ), by operating in the PeakForce Tapping mode. Triangular silicon nitride cantilevers with a nominal spring constant of  $0.7 \text{ N} \cdot \text{m}^{-1}$  were employed (ScanAsyst-Fluid, Bruker AXS). Analysis and processing of AFM images was performed with the WSxM software.<sup>34</sup>

**Mechanical Stability Studies.** The mechanical stability of HA1 pellicles exposed to erosive challenges was studied by AFM scratching at continuously increasing applied loads. Sample preparation mimicked that used for AFM visualization studies. Rectangular silicon nitride levers with a nominal normal spring constant of  $0.7 \text{ N} \cdot \text{m}^{-1}$  (OMCL-RC800PSA, Olympus, Japan) were used in this case.

Briefly, in these experiments the tip of an AFM cantilever was used to scratch pellicles before and after being exposed to erosive challenges. This was done by acquiring sets of two-dimensional scan/images (lateral scan size of  $1 \mu\text{m}$  and tip velocity of  $40 \mu\text{m} \cdot \text{s}^{-1}$ ) on a given spot of the sample. The load force applied by the tip,  $F_L$ , was kept constant during the acquisition of each of the scan/images, but incremented between consecutive ones. The response of the pellicles to the scratch was characterized by the dependence of its

topography (specifically of its roughness as calculated in ref 35) with the load applied by the tip.

**Erosion–pH Monitoring.** An automatic titration system (902 Titrand, Metrohm Nordic AB, Sweden) was used to follow changes in pH induced by dissolution of circular sintered hydroxyapatite disks (diameter 15 mm, height 3 mm, sintered at  $1250^\circ \text{C}$ , relative density of 98%, Swerea, Sweden), from now on HA2 surfaces. HA2 surfaces were coated with nail varnish on the back and lateral sides. Therefore, their exposed 2D area was  $\sim 177 \text{ mm}^2$ . HA2 surfaces were polished as described in ref 36. AFM imaging of polished HA2 surfaces (Supporting Information, section S1) revealed highly planar areas with an average roughness of  $\sim 3 \text{ nm}$ , even though some deep valleys were still present after polishing which, if considered, led to an average roughness of  $\sim 6 \text{ nm}$ .

Both clean (noncoated) and pellicle-coated HA2 surfaces were studied by means of pH monitoring. Initially, HA2 surfaces were cleaned by means of sonication in a 50/50 water/ethanol solution for 10 min followed by plasma cleaning for 5 min. This cleaning procedure was repeated twice. Pellicle coating was performed by immersing the surfaces in human whole saliva for 1 h, followed by extensive rinsing with PBS buffer. pH monitoring experiments were performed by introducing the surfaces in 60 mL of the solution corresponding to each of the tested erosive challenges. The solution was constantly stirred with a propeller stirrer operated at 6 rps. Then, the change in pH resulting from the immersion of the surfaces was constantly monitored for 30 min.

## RESULTS

**Ellipsometry.** Ellipsometry was used to study, in terms of adsorbed amount, the influence of the different erosive challenges on HA1 pellicles. Figure 1 shows representative examples of the time evolution of the adsorbed amount,  $\Gamma$  (dry mass), during (1) pellicle formation from adsorption of whole saliva (0–60 min), (2) rinsing of the pellicle with PBS buffer pH 7.4 for removing loosely attached material (60–110 min), (3) exposure to erosive challenge (Figure 1a, EC1, Figure 1b, EC2, Figure 1c, EC3, 110–150 min), and (4) rinsing of the challenged pellicle with PBS buffer pH 7.4 (150–190 min).

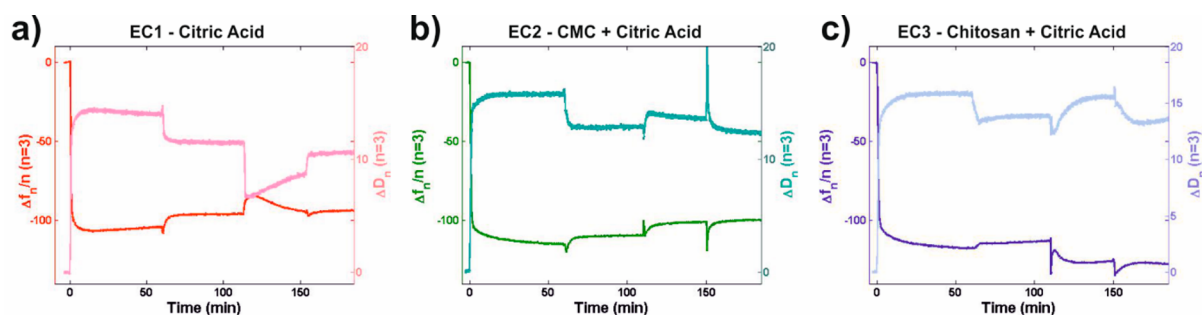


**Figure 2.** Time evolution of frequency and dissipation shifts of the third overtone of HA1 pellicles exposed to (a) EC1, (b) EC2, and (c) EC3 challenges. Data for  $t < 0$  min corresponds to the baseline acquired in PBS buffer. In the time range 0–60 min the HA1 surfaces were in contact with whole saliva leading to the formation of the pellicles. In the time range 60–110 min the pellicles were rinsed with PBS buffer. In the time range 110–150 min the pellicles were exposed to the erosive challenges. Finally, in the time range 150–190 min the challenged pellicles were rinsed again with PBS buffer.

The initial data ( $t < 0$  min) corresponds to the baseline acquired in PBS buffer. The high absorbance/scattering of whole saliva did not allow data acquisition during pellicle formation (0–60 min).

For the analysis of ellipsometry data, we focus on the ratio between the adsorbed amount before and after the exposure of the pellicles to the erosive challenges,  $R_{\text{DryMass}} = \Gamma_{\text{afterEC}} / \Gamma_{\text{beforeEC}}$ . The results obtained were  $R_{\text{DryMass}}(\text{EC1}) = 0.79 \pm 0.01$ ,  $R_{\text{DryMass}}(\text{EC2}) = 0.75 \pm 0.04$ , and  $R_{\text{DryMass}}(\text{EC3}) = 0.83 \pm 0.01$  (Table 1). Thus, exposure of pellicles to all erosive challenges resulted in a decrease of the adsorbed amount. In the case of EC1 (just citric acid), this decrease was  $\sim 21\%$ . Adding CMC to the citric acid solution (EC2) led to a slightly higher decrease, although not statistically significant. Adding chitosan to the citric acid solution (EC3) led to a lower decrease in adsorbed amount, of  $\sim 17\%$ .

**QCM-D.** QCM-D was also used to study the influence of the different erosive challenges on HA1 pellicles (Figure 2). For simplicity, in the analysis of QCM-D data we have focused on the ratio between frequency shifts measured before and after exposure to the erosive challenges,  $R_{\text{WetMass}} = \Delta f_{\text{afterEC}} / \Delta f_{\text{beforeEC}}$ , which is a reasonable estimation of the ratio between the adsorbed wet masses in both situations. For the third overtone, we obtained the following values:  $R_{\text{WetMass}}(\text{EC1}) = 0.98 \pm 0.01$ ,  $R_{\text{WetMass}}(\text{EC2}) = 0.90 \pm 0.01$ , and  $R_{\text{WetMass}}(\text{EC3}) = 1.17 \pm 0.04$ . Thus, exposure of the HA1 pellicles to citric acid (EC1) had no significant effect on the wet mass. When the citric acid solution contained CMC (EC2) the wet mass decreased, whereas if it contained chitosan (EC3) it increased.

QCM-D also provides information on the viscoelasticity of the adsorbed films. This is usually inferred from dissipation shifts. However, it is not straightforward to quantify the viscoelastic character as dissipation shifts are associated not only with the viscoelasticity of the adsorbed material but also with changes in wet mass.<sup>37</sup> Still, a simple way to qualitatively describe the viscoelasticity of the adsorbed material is to analyze the ratio between frequency and dissipation shifts,  $\Delta D / \Delta f$ ,<sup>38</sup> with higher values suggesting a higher viscous character. Specifically, we have compared these ratios before and after the erosive challenges:  $R_{\text{viscoelasticity}} = (\Delta D / \Delta f)_{\text{afterEC}} / (\Delta D / \Delta f)_{\text{beforeEC}}$ . A value of  $R_{\text{viscoelasticity}} > 1$  would indicate that the erosive challenge had increased the viscous character of the pellicle, whereas the opposite would stand for  $R_{\text{viscoelasticity}} < 1$ . For the third overtone, we obtained  $R_{\text{viscoelasticity}}(\text{EC1}) = 1.02 \pm 0.07$ ,  $R_{\text{viscoelasticity}}(\text{EC2}) = 1.03 \pm 0.02$ , and  $R_{\text{viscoelasticity}}(\text{EC3}) = 0.93 \pm 0.05$  (Table 1). Thus, exposing the pellicles to EC1

(citric acid) and to EC2 (CMC in citric acid) challenges led to no significant changes in their viscoelasticity, whereas exposing them to EC3 (chitosan in citric acid) erosive challenge led to less viscous, i.e., more elastic, pellicles.

**AFM Imaging.** AFM topography images of HA1 pellicles before and after being exposed to the different erosive challenges are shown in Figure 3. The images show that

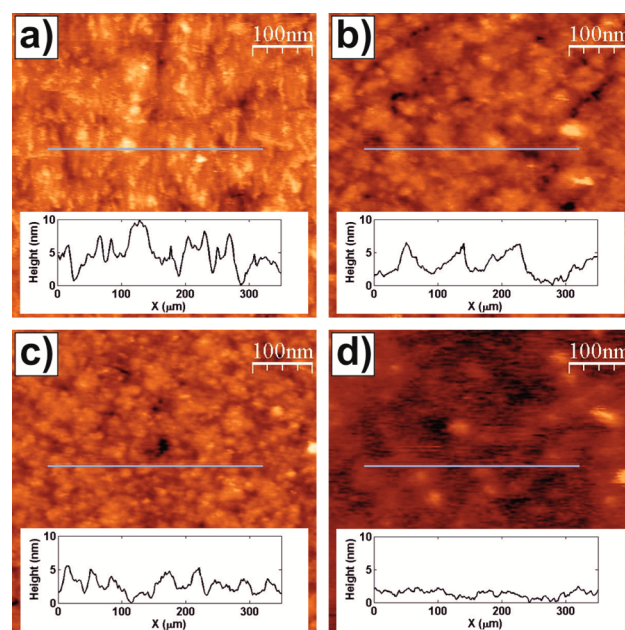


**Figure 3.** Representative AFM images of pellicles in PBS buffer (a) before being exposed to an erosive challenge, and after being exposed to (b) EC1, (c) EC2, and (d) EC3 challenges. Scan area 500 nm × 500 nm. Color height scale 0–17 nm. The images include, as insets, cross-sectional profiles of the surfaces (locations indicated by lines in the topography images).

exposure to EC1 and EC2 erosive challenges lowered the roughness of the pellicles in a similar extent. This effect was significantly more pronounced for pellicles that were exposed to the EC3 erosive challenge.

**Mechanical Stability Studies.** Roughness vs load plots from representative scratching experiments on HA1 pellicles in PBS buffer before and after being exposed to the three different tested erosive challenges are shown in Figure 4.

All (challenged and nonchallenged) pellicles exhibited a similar qualitative response to the scratch. Planar topographies,

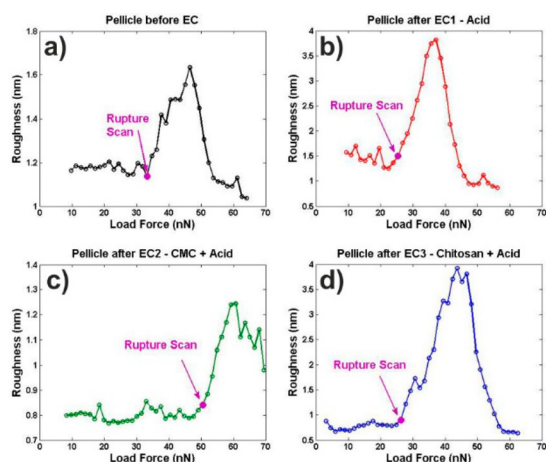


**Figure 4.** Roughness plots corresponding to the scratching of HA1 pellicles (a) before and after being exposed to (b) EC1, (c) EC2, and (d) EC3 challenges.

characterized by a low and homogeneous roughness, were observed at the beginning of each experiment, i.e., for the lowest applied loads. This is indicative of nondestructive sliding of the tip along intact pellicles. When the load was further increased, the pellicles eventually broke as shown by a sudden increase in roughness. The image/scan for which this occurred is highlighted and labeled as “Rupture Scan” for all the plots in Figure 4. We used the load force for which the rupture of the pellicles was observed to characterize their mechanical stability. Specifically, as in the previous sections, we have focused on the ratio between the signal, in this case the load force corresponding to the rupture of the pellicles, before and after the exposure to the erosive challenges,  $R_{\text{strength}} = (\text{RuptureLoad})_{\text{afterEC}} / (\text{RuptureLoad})_{\text{beforeEC}}$ . The results obtained were  $R_{\text{strength}}(\text{EC1}) = 0.78 \pm 0.08$ ,  $R_{\text{strength}}(\text{EC2}) = 1.31 \pm 0.17$ , and  $R_{\text{strength}}(\text{EC3}) = 0.66 \pm 0.06$  (Table 1). Thus, exposure to EC1 (citric acid) and to EC3 (chitosan in citric acid) challenges led to a similar decrease of the mechanical stability of the pellicles (slightly higher for the case of chitosan in citric acid). On the contrary, exposing the pellicles to the EC2 challenge (CMC in citric acid) led to a significant increase of the mechanical stability of the pellicles.

**Erosion–pH Monitoring.** In order to study the effect of the presence of salivary pellicles on the dissolution of HA surfaces exposed to the EC1, EC2, and EC3 challenges, we have monitored changes in pH over time resulting from the immersion of both noncoated and pellicle-coated hydroxyapatite surfaces into solutions corresponding to these challenges.

Upon exposure to citric acid solutions, the dissociated hydrogen ions will dissolve hydroxyapatite by combining with the hydroxyl and phosphate ions on its surface.<sup>3</sup> Overall, this results in an eventual increase of the pH of the erosive solution. Thus, pH variations over time can be used then as a measure of HA dissolution. It is important to consider that HA dissolution and, therefore, pH variations depend on the actual pH value.<sup>39</sup> However, the dissolved amount in our experiments was so small that it led to increments in pH smaller than 0.03 (during the whole experimental time). Therefore, in these experiments it is reasonable to consider HA dissolution rate as pH-independent.

For these experiments we employed HA2 surfaces, i.e., sintered HA disks, rather than HA1 surfaces, i.e., HA-coated QCM-D sensors. This was done in order to be able to identify a

(steady-state) stage of the erosion process which could be unequivocally associated with the dissolution of HA. The hydroxyapatite coating in HA1 surfaces was only 10 nm thick, making it extremely difficult to identify this stage. HA2 surfaces were instead more suitable because of their higher thickness, i.e.,  $\sim 3$   $\mu\text{m}$ .

Representative results are shown in Figure 5. Figure 5a shows the rate of pH variation over time for both noncoated and

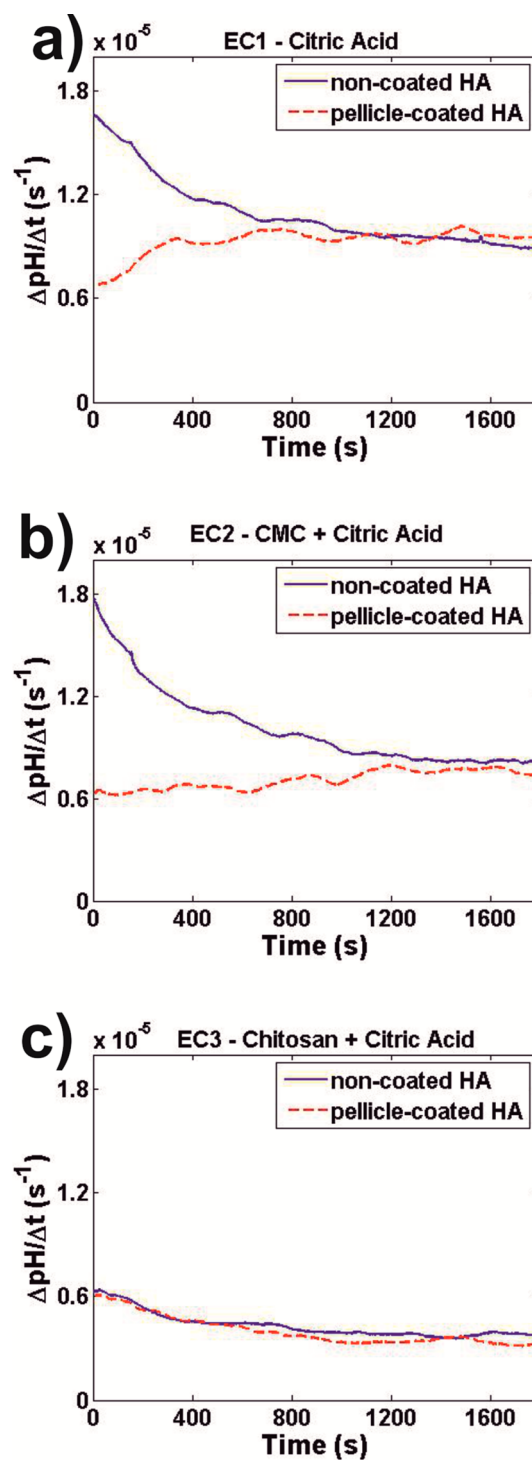


**Figure 5.** Changes in pH over time resulting from the immersion of both noncoated and pellicle-coated HA2 surfaces into solutions corresponding to (a) EC1, (b) EC2, and (c) EC3 challenges.

pellicle-coated HA2 surfaces immersed in the solution corresponding to the erosive challenge EC1 (citric acid 0.3% w/v, initial pH 3.2). We can see how the pH increased (positive rates) immediately after immersion of both samples. However, for the noncoated surfaces the rate diminished gradually with time until a steady state value of  $(8.7 \pm 0.17) \times 10^{-6} \text{ s}^{-1}$  was reached. This initial decrease could be attributed to the fact that some zones of the HA2 surfaces dissolve rapidly just after the exposure of the surface to acid, with later on dissolution proceeding at a slower rate on the whole surface (Supporting Information, section S2). In the case of pellicle-coated HA2 surfaces, just after immersion the initial rate of pH variation was smaller than that observed for the noncoated surfaces. This rate increased with time until the same steady state value as that measured for the noncoated surfaces was achieved after  $\sim 600 \text{ s}$  of exposure to the erosive challenge; i.e., the presence of the pellicle exerted a protective effect for that amount of time.

Figure 5b shows results from representative experiments where the noncoated and pellicle-coated HA2 surfaces were immersed in the solution corresponding to the EC2 challenge (CMC 0.02% w/v solution in citric acid 0.3% w/v, initial pH 3.2). Qualitatively, results are similar to those for surfaces exposed to the EC1 challenge. In this case, the steady state value reached for the rate of pH variation,  $(8.5 \pm 0.37) \times 10^{-6} \text{ s}^{-1}$ , was slightly (but not significantly) smaller. Moreover, the immersion of the pellicle-coated HA2 surfaces led to lower rates of pH variation than those observed of the noncoated surfaces for a significantly longer time,  $\sim 1200 \text{ s}$ , than in the case of the EC1 challenge. Thus, when exposed to the EC2 challenge, the presence of pellicles resulted in a protective effect for approximately twice as long as in the case of the EC1 challenge.

Figure 5c shows results from similar experiments where the noncoated and pellicle-coated HA2 surfaces were immersed in the solution corresponding to the erosive challenge EC3 (chitosan 0.05% w/v solution in citric acid 0.3% w/v, initial pH 3.2). In this case, the noncoated surfaces exhibited a lower rate of pH variation, reaching a steady state value of  $(4.4 \pm 0.30) \times 10^{-6} \text{ s}^{-1}$ . However, for this erosive challenge the role played by the pellicle could not be inferred as results for both the noncoated and the pellicle-coated HA2 surfaces overlapped for the whole experimental time.

Saliva-coated HA2 surfaces were imaged by means of AFM before and after being exposed to the different erosive challenges in pH monitoring experiments (Supporting Information, section S3). This revealed that exposure to the erosive challenges increases the average roughness of the samples by a factor higher than 30. This indicates that pellicles were completely removed from the HA2 surfaces used in pH monitoring experiments. Thus, the loss of the protective effect of the pellicle could be associated with its complete removal.

## DISCUSSION

In this work several surface techniques (ellipsometry, QCM-D, and AFM) were employed to study the interaction between two different polyelectrolytes (one with an anionic character, CMC, and one with a cationic character, chitosan) and salivary pellicles formed on model tooth surfaces. While we have proved these approaches to be highly powerful, they offer as well some limitations. Only in vitro studies are possible. Moreover, the surfaces to be employed have to meet certain characteristics. Highly planar surfaces are needed. Additionally, surfaces for QCM-D studies require a low thickness/mass for

the coating on the quartz crystal, while for ellipsometry studies enough surface reflectance is required. In dental erosion investigations, these requirements are more easily fulfilled by HA than by enamel surfaces. Nevertheless, while enamel is more prone to dissolution than HA,<sup>3</sup> HA is widely accepted as a model surface for in vitro dental erosion studies. However, we have shown that different types of HA surfaces behave differently under exposure to erosive challenges (Supporting Information, section S2). While it is difficult to discuss on the origin of these differences, the fact is that this is not completely unexpected as in vitro erosion experiments are known to yield different results depending on the surfaces and experimental methods employed (e.g., ref 40). In this study, not only different types of HA surfaces were employed, but each type was also studied by means of different experimental techniques. This is highly relevant as different aspects of an experimental technique can also have an influence on HA dissolution, e.g., stirring of the solution (Supporting Information, section S4). Thus, results from in vitro erosion experiments where different types of surfaces and experimental techniques are employed should be carefully interpreted, only in a qualitative way, and implications regarding the in vivo erosion of enamel should be taken with care.

Exposure of HA1 pellicles to the EC1 challenge (citric acid solution) resulted in a decrease of the adsorbed amount provided by ellipsometry. It has been reported that pellicles are permeable to diffusion of calcium and phosphate ions.<sup>41,42</sup> Thus, even though we showed that the pellicle continues to cover the surfaces after being challenged, it should be considered whether the decrease in adsorbed amount could be a consequence of HA dissolving and diffusing through the pellicle. However, it is reasonable to assume that if this occurred, it only did so on a negligible scale as HA1 surfaces could be employed many times in similar experiments yielding similar results. This would have not been possible if HA dissolution was taking place given the low thickness of the HA coating of these surfaces,  $\sim 10 \text{ nm}$ . Thus, the decrease in adsorbed amount suggests the partial desorption of HA1 pellicles exposed to the EC1 challenge. It is difficult to discuss which components primarily account for this observation. It is widely accepted that pellicles are composed of two layers; the innermost layer would be composed mainly of low molecular weight proteins, and the outermost layer would be composed mainly of the long polar/charged mucins.<sup>43</sup> In this scheme, the mechanical stability of the pellicle would be mainly determined by its innermost layer, i.e., that interacting directly with the substrate. The wet mass and the viscoelastic character would in turn be dominated by the outermost pellicle layer. Our results showed that exposure of HA1 pellicles to the EC1 challenge led to a decrease of their mechanical stability, whereas their wet mass and viscoelastic character remained almost unaltered. This suggests that exposure to the EC1 challenge removed mainly low molecular weight proteins from the innermost layer of HA1 pellicles.

pH monitoring experiments of HA2 surfaces immersed in citric acid solution revealed that the presence of a pellicle lowered the rate of pH variation at the beginning of the experiments. However, after  $\sim 10 \text{ min}$  this rate equaled that of noncoated surfaces; i.e., the protective function of the pellicle was lost. Moreover, AFM imaging revealed that the pellicle was completely removed from these surfaces. Thus, pellicles formed on different types of HA surfaces behaved differently upon exposure to erosive challenges. Exposure of HA1 pellicles for 40

min resulted in the loss of a minor part of their dry mass (17–25%, depending on the erosive challenge) and negligible HA1 dissolution, whereas exposure of HA2 pellicles during similar times resulted in the complete removal of the pellicles and substantial HA2 dissolution. It could not be discarded that pellicles formed on HA2 surfaces differ from those formed on HA1 surfaces, and that the former could eventually be completely removed by the erosive solutions leaving the underlying HA2 surfaces undefended against acidic attacks. However, it is more likely that HA2 pellicles resemble HA1 pellicles in the sense that they are not completely removed by the tested acidic solutions. In this case, this observation would just be a consequence of the different tendencies to dissolution of the different HA surfaces. As previously mentioned, it has been reported that pellicles are permeable to diffusion of ions.<sup>41,42</sup> In this scheme the challenged pellicles would act as diffusion barriers for the hydrogen ions that will eventually dissolve the underlying HA. In sintered HA2 surfaces, the attack will take place mainly in the boundaries between the HA granules, which will result in their eventual release (along with the pellicle coating their upper side). Thus, the complete pellicle removal observed in pH monitoring experiments would not be a consequence of the effect of the erosive solution on the pellicle itself, but of the effect of the detachment of the HA granules from the outer surface instead. Due to their lower tendency to dissolution (Supporting Information, section S2), this was not observed in the study of saliva-coated HA1 surfaces. Nevertheless, with this in mind, we hypothesize that it is reasonable to consider for further analysis the results from the experiments performed on both types of HA surfaces. Because of HA dissolution being negligible on the experiments where HA1 surfaces were employed, they can provide insight on how the tested polyelectrolytes would interact with pellicle-coated enamel surfaces in the beginning of *in vivo* erosive challenges. In turn, experiments on the more prone to dissolve HA2 surfaces would give insight on the antierosive performance of the polyelectrolytes.

Exposing HA1 pellicles to citric acid solutions containing either CMC or chitosan (EC2 and EC3 challenges) also led to a decrease in the adsorbed amount provided by ellipsometry. These experiments could be performed many times on the same surfaces yielding similar results. Thus, dissolution of the HA1 coating could be also obviated in these cases. The scenario where the polyelectrolytes would completely replace the pellicles in the experiments performed on HA1 surfaces should also be considered. However, ellipsometry showed that exposing noncoated HA1 surfaces to the EC2 and EC3 challenges resulted in significantly higher adsorbed amounts than those observed for the challenged saliva-coated HA1 surfaces (Supporting Information, section S5). Thus, in these experiments the polyelectrolytes in the citric acid solutions affected the desorption of the pellicles formed on HA1 surfaces, but did not completely remove/replace them.

Exposure of HA1 pellicles to the EC2 challenge (CMC in citric acid) resulted in lower dry and wet masses than exposure to the EC1 challenge (bare citric acid). However, a mere decrease in mass would hardly explain that the exposure to this challenge led to an increase in the mechanical stability of HA1 pellicles. In turn, this suggests that CMC did not just adsorb on top of the challenged pellicles, but penetrated their innermost layer instead. This scheme is supported by AFM images showing no significant differences between the outer surfaces of HA1 pellicles exposed to the EC1 and EC2 challenges. Results

from pH monitoring experiments indicated that the incorporation of CMC into the pellicles led to a significant increase of the time period during which they protected HA2 surfaces from acid-induced dissolution, probably by increasing their effectiveness as ionic diffusion barriers.

Modulation of pellicle desorption, without polyelectrolyte adsorption taking place, was also unlikely the case when HA1 pellicles were exposed to the EC3 challenge (chitosan in citric acid). In this case, the decrease in dry mass was accompanied by a clear increase in wet mass. This suggests that the outer surface of the challenged pellicles contained a higher amount of charged/polar groups, i.e., those that will couple a high amount of solvent. Interaction of chitosan with surface anchored mucins has been well-established.<sup>14,44–46</sup> Thus, the increase in wet mass could be interpreted as the cationic chitosan interacting with, and even cross-linking, the anionic mucins present in the pellicle outermost layer. This scheme is supported (i) by the decrease in the viscous character of HA1 pellicles exposed to this challenge and (ii) by the very low surface roughness of their outer surface revealed by AFM imaging, which is indeed what would be expected for a highly hydrated polymer network. Moreover, this scheme would also explain the small influence of the EC3 challenge on the mechanical stability of the pellicles (given that this aspect is mostly influenced by their innermost layer). However, results from pH monitoring experiments suggest that the interaction between chitosan and HA pellicles has little relevance on the antierosive performance of chitosan-enriched acid solutions. Similar very low rates of pH variations were observed in this case for noncoated and pellicle-coated HA2 surfaces. This similarity was such that it was not possible to identify the transition between the stage where the chitosan-modified pellicle was still on the HA2 surface and the stage where the pellicle was completely removed. This suggests that chitosan modified pellicles and bare chitosan coatings (which would be constantly forming on the HA surface after the acid-induced removal of the pellicle due to the reservoir present in the bulk solution) offer a similar antierosive protective function.

The presented experimental results allow proposing a model on how anionic and cationic polyelectrolytes interact with HA pellicles under acidic conditions, and on how this interaction affects the dissolution of HA itself. The acid solution (citric acid in this work) acts initially by removing part of the adsorbed pellicle, most probably low molecular weight components. Anionic polyelectrolytes (CMC in this work) penetrate the pellicles during their acid-induced removal, prolonging the time period during which the pellicle protects the HA surfaces. The ability of penetrating the pellicles could be a consequence of the anionic polyelectrolytes losing most of their charge under acidic conditions which would also imply a decrease of their effective size. A consequence of the incorporation of CMC into the challenged pellicles is the extension of the time period during which they protect HA surfaces, probably as a result of an increase in their effectiveness as ionic diffusion barriers. However, the low charge of CMC under acidic conditions will also result in a weak interaction with the HA surfaces once the pellicle has been completely removed. This explains the small influence of this polyelectrolyte on bare (noncoated) HA dissolution. Cationic polyelectrolytes (chitosan in this work) would in turn interact with the mucins present in the pellicle outermost layer during their acid-induced removal. It is not possible to conclude from this work whether this prolongs the lifetime of the challenged pellicle, as the presence of chitosan seemed to provide a similar protection toward acid-induced

dissolution to both noncoated and pellicle-coated HA surfaces. Under the specific conditions of the experiments within this work, chitosan offered better antierosive properties than CMC. However, it is well-known that results on this type of studies are highly dependent on the type, concentration, and pH of the acid employed.<sup>3</sup> A dependence on the polymer concentration would also be expected. In this work, we have chosen for comparison values of these aspects similar to those used in previous works, e.g., refs 13 and 14. Moreover, interindividual differences in the composition of the salivary pellicles might also play a role. The influence of these aspects should be addressed in future studies.

## CONCLUSIONS

This work demonstrates the versatility of combining different nonlabeling surface techniques (ellipsometry, QCM-D, and AFM) in the study of the interaction between polyelectrolytes of diverse ionic character and HA pellicles under acidic conditions. Moreover, this work shows as well how such information is fundamental in understanding how the presence of these polyelectrolytes in the acid solutions affects HA dissolution.

We have shown that exposure to acidic erosive challenges results in the removal of a minor fraction of HA pellicles. Nevertheless, the challenged pellicles exert a time-limited protective function on HA against acid-induced dissolution, probably because they act as ionic diffusion barriers.

If the acidic erosive solution includes CMC, an anionic polyelectrolyte, the CMC molecules penetrate the challenged pellicles prolonging in time the protection they offer HA against acid-induced dissolution. However, the CMC films that form on HA surfaces after the complete removal of the modified pellicles offer a weak protection against HA dissolution. This is attributed to the anionic polyelectrolyte losing almost all its charge under acidic conditions, which leads to weak interactions with HA.

Our results also suggest that when chitosan, a cationic polyelectrolyte, is present in the acidic erosive solution, it does not penetrate exposed HA pellicles, but adsorbs on top of them instead. However, this has a very limited influence on HA dissolution, as we have shown that chitosan-modified pellicles have a similar effect on HA dissolution as the chitosan coatings that form on the HA surfaces after the complete acid-induced removal of the modified pellicles. Beside this similarity, the protection offered to HA against dissolution at both stages was notably higher than that offered by the anionic CMC.

## ASSOCIATED CONTENT

### Supporting Information

The Supporting Information is available free of charge on the ACS Publications website at DOI: 10.1021/acsami.5b07118.

AFM imaging of polished HA2 surfaces, HA1 and HA2 surfaces in citric acid solution, and saliva-coated HA2 surfaces before and after being exposed to an erosive challenge; effect of stirring rate in dissolution of HA2 surfaces studied by pH monitoring; ellipsometry investigations of noncoated HA1 surfaces exposed to EC2 and EC3 challenges (PDF)

## AUTHOR INFORMATION

### Corresponding Author

\*E-mail: javier.sotres@mah.se.

## Notes

The authors declare no competing financial interest.

## ACKNOWLEDGMENTS

Financial support from the Crafoord Foundation (Grant 20140640) and from Malmö University is gratefully acknowledged. Thomas Arnebrant acknowledges the Gustaf Th. Ohlsson Foundation, and Liselott Lindh acknowledges the Swedish Laryng Foundation (Grant 20/10) for financial support.

## ABBREVIATIONS

HA, hydroxyapatite  
CMC, carboxymethyl cellulose  
QCM-D, quartz crystal microbalance with dissipation  
AFM, atomic force microscopy  
PBS, phosphate-buffered saline

## REFERENCES

- (1) Bartlett, D. W. The Role of Erosion in Tooth Wear: Aetiology, Prevention and Management. *Int. Dent. J.* **2005**, *55*, 277–284.
- (2) Johansson, A. K.; Lingström, P.; Birkhed, D. Comparison of Factors Potentially Related to the Occurrence of Dental Erosion in High- and Low-Erosion Groups. *Eur. J. Oral Sci.* **2002**, *110*, 204–211.
- (3) Featherstone, J. D. B.; Lussi, A. Understanding the Chemistry of Dental Erosion. *Monogr. Oral Sci.* **2006**, *20*, 66–76.
- (4) Hara, A. T.; Lussi, A.; Zero, D. T. Biological Factors. *Monogr. Oral Sci.* **2006**, *20*, 88–99.
- (5) Hannig, M.; Hannig, C. The Pellicle and Erosion. *Monogr. Oral Sci.* **2014**, *25*, 206–214.
- (6) Gambon, D. L.; Brand, H. S.; Veerman, E. C. I. Dental Erosion in the 21st Century: What Is Happening to Nutritional Habits and Lifestyle in Our Society? *Br. Dent. J.* **2012**, *213*, 55–57.
- (7) Dugmore, C. R.; Rock, W. P. The Progression of Tooth Erosion in a Cohort of Adolescents of Mixed Ethnicity. *Int. J. Paediatr. Dent.* **2003**, *13*, 295–303.
- (8) El Aidi, H.; Bronkhorst, E. M.; Huysmans, M. C. D. N. J. M.; Truin, G.-J. Dynamics of Tooth Erosion in Adolescents: A 3-Year Longitudinal Study. *J. Dent.* **2010**, *38*, 131–137.
- (9) Ganss, C.; Klimek, J.; Giese, K. Dental Erosion in Children and Adolescents - a Cross-Sectional and Longitudinal Investigation Using Study Models. *Community Dent. Oral. Epidemiol.* **2001**, *29*, 264–271.
- (10) Nunn, J. H.; Gordon, P. H.; Morris, A. J.; Pine, C. M.; Walker, A. Dental Erosion - Changing Prevalence? A Review of British National Childrens' Surveys. *Int. J. Paediatr. Dent.* **2003**, *13*, 98–105.
- (11) Tahmassebi, J. F.; Duggal, M. S.; Malik-Kotru, G.; Curzon, M. E. J. Soft Drinks and Dental Health: A Review of the Current Literature. *J. Dent.* **2006**, *34*, 2–11.
- (12) Grenby, T. H. Lessening Dental Erosive Potential by Product Modification. *Eur. J. Oral Sci.* **1996**, *104*, 221–228.
- (13) Barbour, M. E.; Shellis, R. P.; Parker, D. M.; Allen, G. C.; Addy, M. An Investigation of Some Food-Approved Polymers as Agents to Inhibit Hydroxyapatite Dissolution. *Eur. J. Oral Sci.* **2005**, *113*, 457–461.
- (14) Lee, H.-S.; Tsai, S.; Kuo, C.-C.; Bassani, A. W.; Pepe-Mooney, B.; Miksa, D.; Masters, J.; Sullivan, R.; Composto, R. J. Chitosan Adsorption on Hydroxyapatite and Its Role in Preventing Acid Erosion. *J. Colloid Interface Sci.* **2012**, *385*, 235–243.
- (15) Nongonierma, A. B.; Fitzgerald, R. J. Biofunctional Properties of Caseinophosphopeptides in the Oral Cavity. *Caries Res.* **2012**, *46*, 234–267.
- (16) Valentijn-Benz, M.; van 't Hof, W.; Bikker, F. J.; Nazmi, K.; Brand, H. S.; Sotres, J.; Lindh, L.; Arnebrant, T.; Veerman, E. C. I. Sphingoid Bases Inhibit Acid-Induced Demineralization of Hydroxyapatite. *Caries Res.* **2015**, *49*, 9–17.



- (17) White, A. J.; Gracia, L. H.; Barbour, M. E. Inhibition of Dental Erosion by Casein and Casein-Derived Proteins. *Caries Res.* **2011**, *45*, 13–20.
- (18) Rodahl, M.; Höök, F.; Fredriksson, C.; Keller, C. A.; Krozer, A.; Brzezinski, P.; Voinova, M.; Kasemo, B. Simultaneous Frequency and Dissipation Factor QCM Measurements of Biomolecular Adsorption and Cell Adhesion. *Faraday Discuss.* **1997**, *107*, 229–246.
- (19) Sauerbrey, G. Verwendung von Schwingquarzen zur Wägung Dünner Schichten und zur Mikrowägung. *Eur. Phys. J. A* **1959**, *155*, 206–222.
- (20) Reviakine, I.; Johannsmann, D.; Richter, R. P. Hearing What You Cannot See and Visualizing What You Hear: Interpreting Quartz Crystal Microbalance Data from Solvated Interfaces. *Anal. Chem.* **2011**, *83*, 8838–8848.
- (21) Höök, F.; Kasemo, B.; Nylander, T.; Fant, C.; Sott, K.; Elwing, H. Variations in Coupled Water, Viscoelastic Properties, and Film Thickness of a Mefp-1 Protein Film During Adsorption and Cross-Linking: A Quartz Crystal Microbalance with Dissipation Monitoring, Ellipsometry, and Surface Plasmon Resonance Study. *Anal. Chem.* **2001**, *73*, 5796–5804.
- (22) Sotres, J.; Barrantes, A.; Lindh, L.; Arnebrant, T. Strategies for a Direct Characterization of Phosphoproteins on Hydroxyapatite Surfaces. *Caries Res.* **2014**, *48*, 98–110.
- (23) Rodahl, M.; Höök, F.; Krozer, A.; Brzezinski, P.; Kasemo, B. Quartz Crystal Microbalance Setup for Frequency and Q-Factor Measurements in Gaseous and Liquid Environments. *Rev. Sci. Instrum.* **1995**, *66*, 3924–3930.
- (24) Jensen, T. *Development of a Novel Biomaterial: A Nanotechnological Approach*. Ph.D. Thesis, University of Aarhus, Aarhus, Denmark, 2009.
- (25) Azzam, R. M. A.; Bashara, N. M. *Ellipsometry and Polarized Light*; North-Holland: Amsterdam, 1977.
- (26) Cuypers, P. A. *Dynamic Ellipsometry: Biochemical and Biomedical Applications*. Ph.D. Thesis, Rijksuniversiteit Limburg, Maastricht, The Netherlands, 1976.
- (27) Landgren, M.; Jönsson, B. Determination of the Optical Properties of Si/SiO<sub>2</sub> Surfaces by Means of Ellipsometry Using Different Ambient Media. *J. Phys. Chem.* **1993**, *97*, 1656–1660.
- (28) Cuypers, P. A.; Corsel, J. W.; Janssen, M. P.; Kop, J. M.; Hermens, W. T.; Hemker, H. C. The Adsorption of Prothrombin to Phosphatidylserine Multilayers Quantitated by Ellipsometry. *J. Biol. Chem.* **1983**, *258*, 2426–2431.
- (29) Stenberg, M.; Nygren, H. The Use of the Isoscope Ellipsometer in the Study of Adsorbed Proteins and Biospecific Binding Reactions. *J. Phys. Colloques* **1983**, *44*, C10-83–C10-86.
- (30) Tiberg, F. Physical Characterization of Non-Ionic Surfactant Layers Adsorbed at Hydrophilic and Hydrophobic Solid Surfaces by Time-Resolved Ellipsometry. *J. Chem. Soc., Faraday Trans.* **1996**, *92*, 531–538.
- (31) Tiberg, F.; Landgren, M. Characterization of Thin Nonionic Surfactant Films at the Silica/Water Interface by Means of Ellipsometry. *Langmuir* **1993**, *9*, 927–932.
- (32) de Feijter, J. A.; Benjamins, J.; Veer, F. A. Ellipsometry as a Tool to Study Adsorption Behavior of Synthetic and Biopolymers at Air-Water Interface. *Biopolymers* **1978**, *17*, 1759–1772.
- (33) Cárdenas, M.; Arnebrant, T.; Rennie, A.; Fragneto, G.; Thomas, R. K.; Lindh, L. Human Saliva Forms a Complex Film Structure on Alumina Surfaces. *Biomacromolecules* **2007**, *8*, 65–69.
- (34) Horcas, I.; Fernández, R.; Gómez-Rodríguez, J. M.; Colchero, J.; Gómez-Herrero, J.; Baró, A. M. WSxM: A Software for Scanning Probe Microscopy and a Tool for Nanotechnology. *Rev. Sci. Instrum.* **2007**, *78*, 013705.
- (35) Sotres, J.; Barrantes, A.; Arnebrant, T. Friction Force Spectroscopy as a Tool to Study the Strength and Lateral Diffusion of Protein Layers. *Langmuir* **2011**, *27*, 9439–9448.
- (36) Santos, O.; Lindh, L.; Halthur, T.; Arnebrant, T. Adsorption from Saliva to Silica and Hydroxyapatite Surfaces and Elution of Salivary Films by SDS and Delmopinol. *Biofouling* **2010**, *26*, 697–710.
- (37) Voinova, M. V.; Rodahl, M.; Jonson, M.; Kasemo, B. Viscoelastic Acoustic Response of Layered Polymer Films at Fluid-Solid Interfaces: Continuum Mechanics Approach. *Phys. Scr.* **1999**, *59*, 391.
- (38) Vickinge, T. P.; Hansson, K. M.; Sandström, P.; Liedberg, B.; Lindahl, T. L.; Lundström, I.; Tengvall, P.; Höök, F. Comparison of Surface Plasmon Resonance and Quartz Crystal Microbalance in the Study of Whole Blood and Plasma Coagulation. *Biosens. Bioelectron.* **2000**, *15*, 605–613.
- (39) Thomann, J. M.; Voegel, J. C.; Gramain, P. Kinetics of Dissolution of Calcium Hydroxyapatite Powder. III: pH and Sample Conditioning Effects. *Calcif. Tissue Int.* **1990**, *46*, 121–129.
- (40) Elton, V.; Cooper, L.; Higham, S. M.; Pender, N. Validation of Enamel Erosion in Vitro. *J. Dent.* **2009**, *37*, 336–341.
- (41) Hannig, M.; Joiner, A. The Structure, Function and Properties of the Acquired Pellicle. *Monogr. Oral Sci.* **2006**, *19*, 29–64.
- (42) Zahradnik, R. T.; Moreno, E. C.; Burke, E. J. Effect of Salivary Pellicle on Enamel Subsurface Demineralization in Vitro. *J. Dent. Res.* **1976**, *55*, 664–670.
- (43) Lindh, L.; Aroonsang, W.; Sotres, J.; Arnebrant, T. Salivary Pellicles. *Monogr. Oral Sci.* **2014**, *24*, 30–39.
- (44) Dédinaite, A.; Lundin, M.; Macakova, L.; Auletta, T. Mucin–Chitosan Complexes at the Solid–Liquid Interface: Multilayer Formation and Stability in Surfactant Solutions. *Langmuir* **2005**, *21*, 9502–9509.
- (45) Pettersson, T.; Dédinaite, A. Normal and Friction Forces between Mucin and Mucin–Chitosan Layers in Absence and Presence of SDS. *J. Colloid Interface Sci.* **2008**, *324*, 246–256.
- (46) Svensson, O.; Thuresson, K.; Arnebrant, T. Interactions between Chitosan-Modified Particles and Mucin-Coated Surfaces. *J. Colloid Interface Sci.* **2008**, *325*, 346–350.